J|A|C|S
ARTICLES

Published on Web 12/18/2008

Mechanism of Very Large Scale Assembly of SWNTs in Template Guided Fluidic Assembly Process

Laila Jaber-Ansari, Myung Gwan Hahm, Sivasubramanian Somu, Yolanda Echegoyen Sanz, Ahmed Busnaina, and Yung Joon Jung*

Department of Mechanical and Industrial Engineering, Northeastern University, Boston, Massachusetts 02115

Received September 26, 2008; E-mail: jungy@coe.neu.edu

Abstract: Very large scale patterned single-walled carbon nanotube (SWNT) networks were fabricated using a newly developed template guided fluidic assembly process. A mechanism for SWNT assembly and their control is described here. To maximize the directed assembly efficiency of SWNTs toward a wafer level SWNT deposition, Si or SiO_2 substrate was pretreated with precisely controlled SF_6, O_2, and Ar plasma. Chemical and physical properties of the surface were characterized using several surface characterization techniques to investigate and control the mechanism of SWNT assembly. We found that hydrophilic chemical groups such as hydroxides were created on the silicon or silicon oxide surface through the controlled plasma treatment and fluidic SWNT dip-coating process. Also we found that nanoscale rough surface structures formed during the plasma treatment significantly increased the number of dangling bonds and hydroxide functional groups on the surface. These combined chemical and physical enhancements that attract SWNTs in the aqueous solution enable us to build highly organized and very large scale SWNT network architectures effectively in various dimensions and geometries.

Carbon nanotubes (CNTs) are promising candidates for the use as components in nanoscale electronics[1,2] and electromechanical devices[3−6] due to their superior mechanical properties, high electron mobility, large current capability, and unique one-dimensional nanostructure. In order to implement these applications, it is essential to develop a simple and reliable manufacturing process that controllably assembles CNTs in desired locations with controlled orientations, and nanoscale dimensions over a large area. A few approaches have been reported the assembly of SWNTs using chemical vapor deposition (CVD),[7−10] chemical functionalization,[11,12] electrophoretic deposition (EPD), or dielectrophoresis (DEP).[12−14] CVD is an effective method to directly synthesize CNTs at the desired locations on a substrate by patterning catalyst materials. But its high temperature process (500−900 °C) and difficulty in controlling the growth direction and the density of CNTs significantly limits its effectiveness, especially for electronic device applications. EDP has an advantage of fabricating highly oriented nanotubes between electrodes, but it is effective only within local areas where the electric-field is at maximum. Recently, we have demonstrated the liquid-phase fabrication of highly organized SWNT lateral network architectures.[15] In this method using a lithographically patterned template assisted dip-coating, SWNTs were directly assembled on a hydrophilic surface, between predesigned photoresist channels, forming organized SWNT lateral networks in diverse geometries with feature sizes ranging from 100 nm to 10 μm. The fluidic assembly of SWNTs can be improved when the substrates are pretreated with plasma and followed by deionized water flush resulting in enhanced hydrophilic behavior. The level of control provided by this method enable us to construct complex SWNT architectures, which could fulfill their potential applications such as active elements in transistors, horizontal interconnect systems, and sensors. However there has been no clear explanation for the mechanism of this site selective assembly of SWNTs and the control for the very large scale assembly. Here we report the results of a study that clearly elucidate the role of chemical

(1) Avouris, P.; Chen, Z.; Perebeinos, V. *Nat. Nanotech.* **2006**, *2*, 605–615.
(2) Portnoi, M. E.; Kibis, O. V.; Rosenau da Costa, M. *Superlat. Microstruct.* **2008**, *43*, 399–407.
(3) Hayamizu, Y.; Yamada, T.; Mizuno, K.; Davis, R. C.; Futaba, D. N.; Yumura, M.; Hata, K. *Nat. Nanotech.* **2008**, *3*, 289–294.
(4) Suppiger, D.; Busato, S.; Ermanni, P. *Carbon* **2008**, *46*, 1085–1090.
(5) Hierold, C.; Jungen, A.; Stampfer, C.; Helbling, T. *Sens. Actuators, A* **2007**, *136*, 51–61.
(6) Kang, J. W.; Lee, J. H.; Lee, H. J.; Hwang, H. *J. Phys. E* **2005**, *27*, 332–340.
(7) Jung, Y. J.; Homma, Y.; Ogino, T.; Kobayashi, Y.; Takagi, D.; Wei, B. Q.; Vajtai, R.; Ajayan, P. M. *J. Phys. Chem. B* **2003**, *107*, 6859–6864.
(8) Hata, K.; Futaba, D. N.; Mizuno, K.; Namai, T.; Yumura, M.; Iijima, S. *Science* **2004**, *306*, 1362–1364.
(9) Wei, B. Q.; Vajtai, R.; Jung, Y.; Ward, J.; Zhang, R.; Ramanath, G.; Ajayan, P. M. *Nature* **2002**, *416*, 495–496.
(10) Casell, A. M.; Raymaskers, J. A.; Kong, J.; Dai, H. *J. Phys. Chem. B* **1999**, *103*, 6484–6492.
(11) Lee, M.; Im, J.; Lee, B. Y.; Myung, S.; Kang, J.; Huang, L.; Kwon, Y.-K.; Hong, S. *Nat. Nanotech.* **2006**, *1*, 66–71.
(12) Kamat, P. V.; Thomas, K. G.; Barazzouk, S.; Girishkumar, G.; Vinodgopal, K.; Meisel, D. *J. Am. Chem. Soc.* **2004**, *126*, 10757–10762.
(13) Makaram, P.; Somu, S.; Xiong, X.; Busnaina, A.; Jung, Y. J.; McGruer, N. *Appl. Phys. Lett.* **2007**, *90*, 243108(1−3).
(14) Makaram, P.; Selvarasah, S.; Xiong, X.; Chen, C.-L.; Busnaina, A.; Khanduja, N.; Dokmeci, M. R. *Nanotechnology* **2007**, *18*, 395204(1−5).
(15) Xiong, X.; Jaber-Ansari, L.; Hahm, M. G.; Busnaina, A.; Jung, Y. J. *Small* **2007**, *3*, 2006–1010.

10.1021/ja8076523 CCC: $40.75

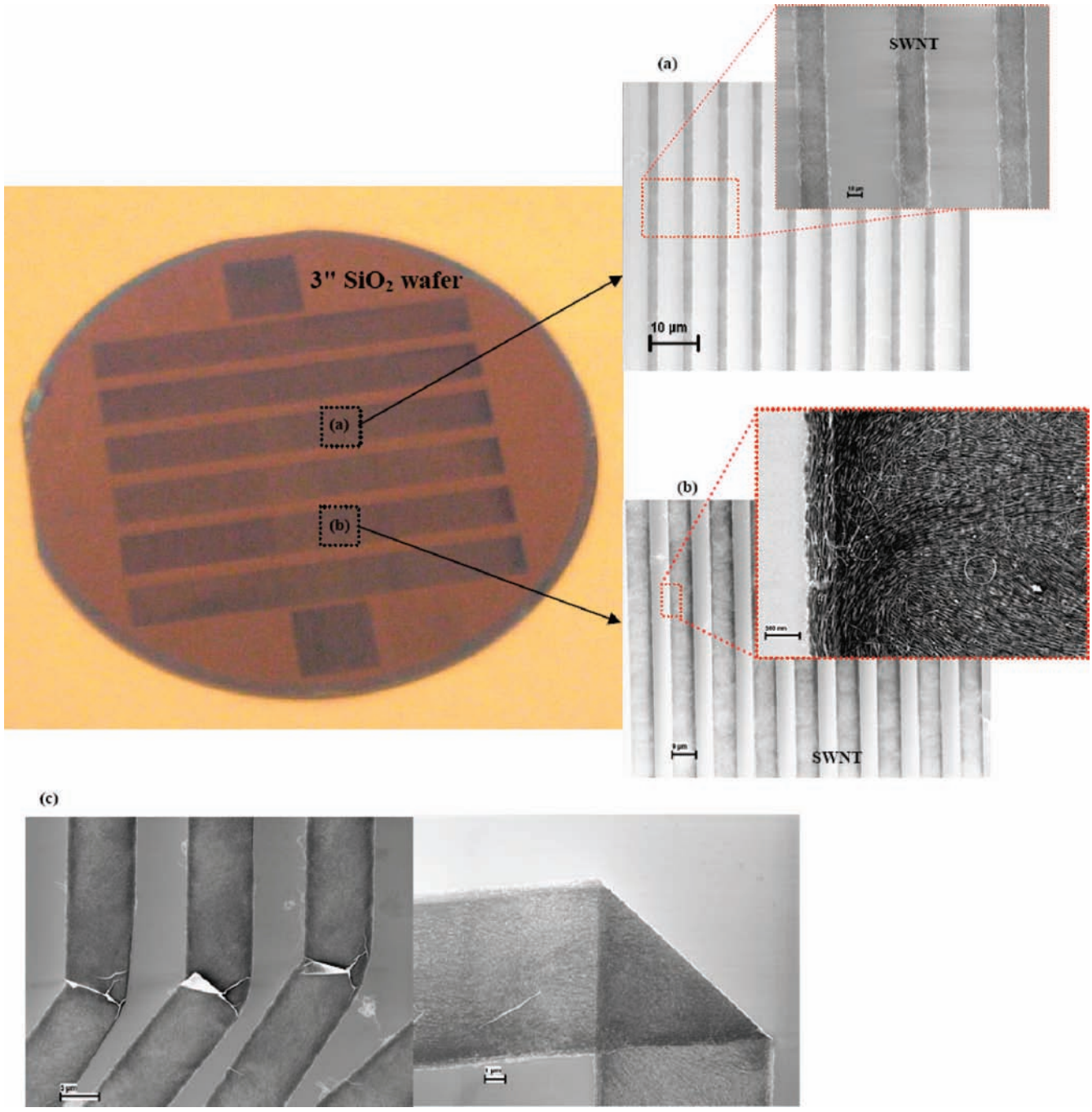

Figure 1. SEM images of the assembled SWNT structures in the 3 in. wafer with pattern widths of (a) 3 μm, (b) 9 μm, and (c) bent and folded structures of assembled SWNTs showing the robustness of these structures.

and physical surface properties for the assembly of SWNTs and their control toward building highly organized SWNT network architectures on a wafer level.

For the assembly of SWNTs into horizontally organized network architectures, we used 0.23 wt% SWNT-deionized (DI) water solution (obtained from Nantero Inc.) with the SWNT's length of 2−3 μm. The utilized SWNTs were terminated with carboxylic acid groups partially dissociate into H^+ cations and COO^- anions in the aqueous solution leading to the presence of a net negative charge on the surface of SWNTs. In order to improve the contact between the SWNT-deionized water solution and substrate, the substrate was pretreated using an Inductively-Coupled Plasma (ICP) with mixed gas flow of O_2 (20 sccm), SF_6 (20 sccm) and Ar (5 sccm). Then a photo/e-beam resist film on the Si or SiO_2 substrate was patterned using optical or electron-beam lithography techniques and vertically submerged into the SWNT solution using a dip-coater and then gradually lifted from the solution with a constant pulling speed, 0.1 mm/sec. To characterize physical properties of the template surface and their role in SWNT assembly, Scanning electron microscopy (SEM), Raman spectroscopy, and Atomic force microscopy (AFM) were used. To investigate chemical properties of template surface and their role for SWNT assembly, a contact angle measurement system and X-ray photoelectron spectroscopy (XPS) were employed.

Figure 1 is a representative of optical and SEM images of patterned SWNT network structures fabricated on the 3 in. wafer using aforementioned template guided fluidic assembly process.

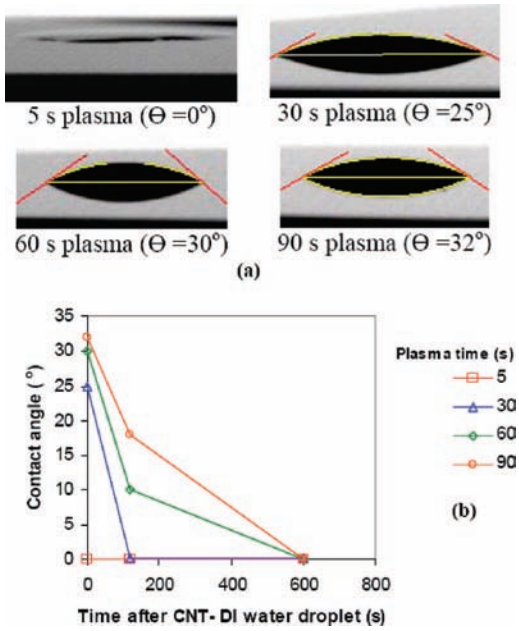

Figure 2. (a) Contact angle (Θ) measurement of Si substrate after 5, 30, 60, and 90 s of SF_6/O_2/Ar plasma treatment. (b) Contact angle change vs time on the same substrates.

It is clearly seen that SWNTs are assembled only on open areas such as Si or SiO_2 (negative patterns of photoresist) and form highly organized arrays precisely occupying predesigned shapes and sizes (1 μm−10 μm). One of the most important features of our developed assembly process is that effective micro- and nanoscale SWNT assembly resulting in very large scale SWNT network architectures is accomplished using a simple dry plasma treatment to change the surface property of patterned silicon or silicon dioxide substrates into hydrophilic without the need to resort to complex wet chemical functionalization processes. Figure 1c shows the assembled SWNTs demonstrating a robust network that can be bent or folded without damaging their assembled structures (SWNT networks in this Figure were bent and folded by strong blow-drying with nitrogen gas). It also indicates that patterned SWNT networks do not have a very strong bonding with the substrate and can be removed easily. It is assumed that the bonds between SWNTs and the hydroxyl groups are breaking during the bending/folding of SWNTs since the remaining surface of silicon or silicon oxide show the hydrophilic behavior of SWNT-DI water solution even after removing assembled SWNT structures. Therefore they show strong potential to be transferred to other substrates.

The first step toward selective assembly of SWNTs is to produce appropriate sites on the substrate that can attract the SWNT solution selectively. Since we used a SWNT-DI water aqueous solution, one of the main issues was the wetting ability of this solution for our particular substrate. The initial contact angle measurement of SWNT-DI water solution on the untreated silicon and silicon dioxide surfaces were 36 and 30°, respectively.[15] Our experiment result showed that plasma treatment of the substrate in a mixed gas flow of O_2 (20 sccm), SF_6 (20 sccm), and Ar (5 sccm) can improve interaction between the substrate and the SWNT-DI water solution drastically. Figure 2a shows the results of the contact angle (Θ) measurement right after dropping the SWNT-DI water solution on silicon substrates treated with plasma for times (5, 30, 60, and 90 s). The lowest contact angle (the best hydrophilic behavior) of SWNT solution was obtained with 5 s plasma etched silicon substrate (0°) and

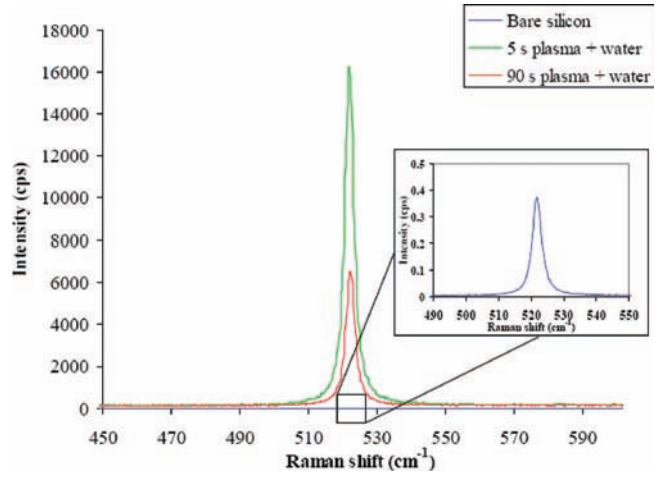

Figure 3. Raman shifts of 5 and 90 s plasma treated Si substrates after 5 min rinse in water showing the enhanced Raman peaks resulting from plasma treatment. The inset shows the magnified Raman peak of the untreated silicon substrate.

the contact angle increased as the plasma etching time increased. However, given enough time, the contact angle between all silicon substrates and SWNT solution gradually changed to 0°. Figure 2b shows the change of the contact angle with the time after depositing a droplet of the SWNT solution on these substrates. The result indicates that the 5 s plasma etched sample changes instantly to a completely hydrophilic surface while it takes more time to produce hydrophilic groups for the longer plasma etched silicon substrates.

To characterize the nature of the Si surface changes as a result of plasma treatment further, we used Raman spectroscopy with a 443 nm line of HeNe 20 mW laser for excitation on these plasma treated substrates. Figure 3 shows Raman bands of bare and plasma treated (5 and 90 s) silicon. The maximum intensity in Silicon Raman spectra was achieved after 5 s plasma treatment. The enhanced Raman scattering from silicon surface of different structures has been reported in the literature[16−18] Baroult et al. performed in situ Raman on silicon substrate subjected to SF_6/Ar plasma and they reported enhanced Si Raman peak as the result of roughness due to plasma treatment.[19] The enhancement of Si peak (at 521 cm^{-1}) can be explained by electromagnetic cavity resonance as a result of the matching of the frequency of the incident field with that of an electromagnetic eigenmode of the surface particles, leading to an increase in both inelastic and elastic scatterings.[18] SEM and AFM results for the 5 and 90 s plasma treated Si surfaces are shown in Figure 4. The 5 s plasma etched sample (Figure 4b1) shows nanostructures on the surface of silicon were 50 nm wide and 5 nm high, but the 90 s plasma etched sample (Figure 4c1) shows surface structures around 400 nm wide with a height variation of about 5 nm over that area whereas in bare silicon the surface protuberances are only 100−200 Å deep. These surface structures can be seen as the grain shaped domains in the SEM images (Figure 4b2 and c2). These results are in complete agreement with Raman spectra showing an enormous

(16) Murphy, D. V.; Brueck, S. R. J. *Opt. Lett.* **1983**, *8*, 494–496.
(17) Zaidi, S. H.; Chu, A.; Brueck, S. R.; J., *J. Appl. Phys.* **1996**, *80*, 6997–7008.
(18) Liu, F. M.; Ren, B.; Wu, J. H.; Yan, J. W.; Xue, X. F.; Mao, B. W.; Tian, Z. Q. *Chem. Phys. Lett.* **2003**, *382*, 502–507.
(19) Brault, P.; Mathias, J.; Laure, C.; Ranson, P.; Texier, O. *J. Phys.: Condens. Matter* **1994**, *6*, L1–L6.

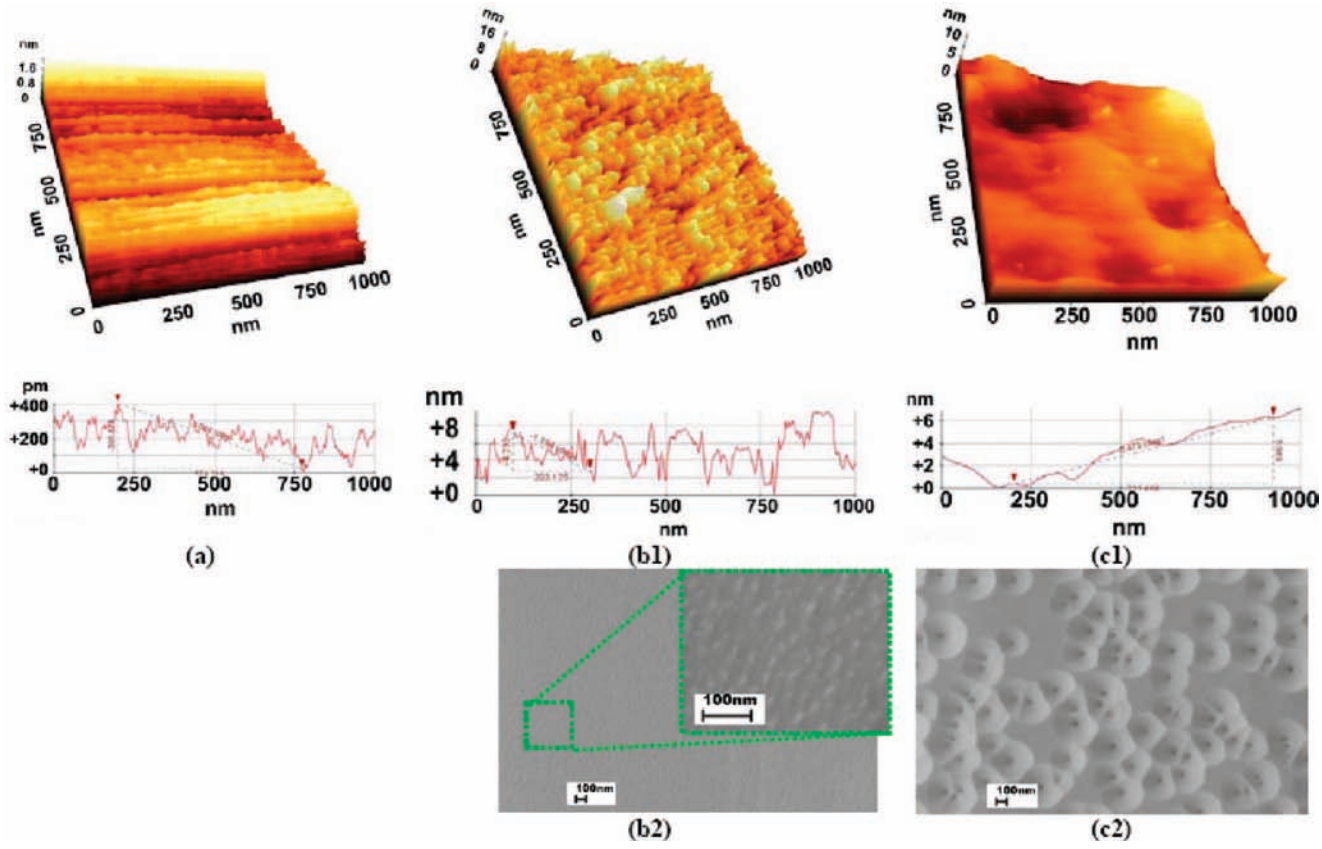

Figure 4. Effect of plasma treatment on the surface morphology of Si (a) AFM image of a 1 μm × 1 μm area of bare Si, (b1) AFM image of a 1 μm × 1 μm area of 5 s plasma treated Si, (b2) SEM image of 5 s plasma treated Si, (c1) AFM image of a 1 μm × 1 μm area of 90 s plasma treated Si and (c2) SEM image of 5 s plasma treated Si.

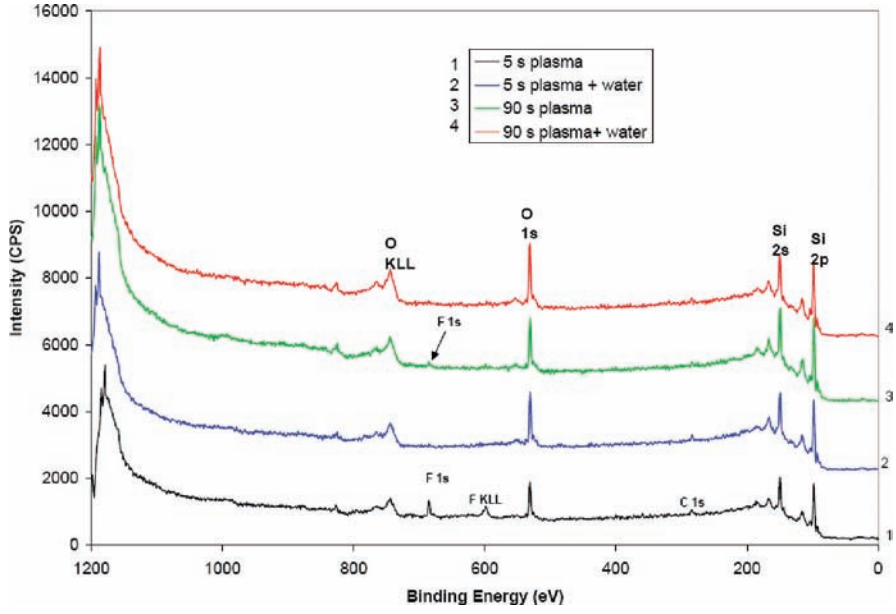

Figure 5. Large XPS spectrum of 5 and 90 s $SF_6/Ar/O_2$ plasma etched silicon before and after water treatment. The fluorine peak that is observed after plasma treatment, vanishes with rinsing the sample in water.

increase in roughness after 5 s plasma etching treatment (Figure 4b1 and b2) and then a diminishing of the surface roughness with further etching of the substrate (Figure 4c1 and c2).

Although the Raman and AFM results show an increase in the physical activity of the plasma treated substrates, such as enhanced roughness, the nature of the chemical functional groups that are produced as the result of plasma treatment remains unclear. To acquire a better understanding of the latter, we performed XPS on the plasma etched silicon surface. The XPS experiments were performed on a KRATOS Analytical spectrometer using Mg Kα (1253.6 eV). Narrow scan spectra of all regions of interest were recorded with 160 eV pass energy

in order to identify the elemental bonding states. Figure 5 shows a large XPS spectrum acquired with low resolution of plasma etched and water treated silicon substrate. The XPS analysis shows that the surface layer of samples after exposure to SF_6/Ar/O_2 plasma consists mainly of silicon, oxygen and fluorine and a small amount of carbon. Analysis of silicon XPS required correction of spectral energy scale due to specimen charging. The binding energy was aligned such that the C 1s line from adventitious carbon contamination is at 284.8 eV. The fluorine amount at the surface after plasma treatment is much larger for the 5 s plasma treated sample (about 7% of surface atoms) compared with 90 s plasma treated silicon (less than 1% of surface atoms). The fact that fluorine peaks vanish after rinsing in water for both samples shows that the Si−F bonds that formed are easily replaced by Si−OH groups in the presence of water. The F terminated surface is electrically polarized, and the water molecule is also polar. Hence, the interaction of the H−OH with the F-terminated surface results in the formation of a stable adsorption structure due to the Coulomb attraction between the H atom of the water and the F atom on the surface. This leads to the breaking of the Si−F bond and the formation of the Si−O bond. This replacement can be observed in the XPS spectra where the fluorine disappearance is correlated with the increase in the intensity of oxygen peaks in the water treated sample. The narrow scan spectra of the Si 2p showed that Si−O, SiO_2 and Si−F bonds exist on the surface of the silicon after plasma treatment. The 90 s plasma etched sample however has less Si−F bonds since Figure 5 shows a small amount of fluorine existing on its surface. After rinsing these samples in DI water, the SiO_2 peak (around 104 eV) shifts to a much lower binding energy which shows incomplete bonding of silicon with oxygen or hydrogen (Figure S1a−d, Supporting Information). To discover the exact nature of these bondings the O 1s spectra for both 5 and 90 s plasma treated samples after rinsing in water was obtained (Figure S2, Supporting Information). The 90 s plasma treated and rinsed sample shows only one peak with a binding energy of SiO_2 (around 533 eV) but the O 1s peak for 5 s plasma etched and rinsed sample can be deconvoluted into Si−O−Si, Si−OH and SiO_2 peaks. This shows that a lot of dangling bonds exist on the surface of this substrate along with hydrophilic OH^- groups and hence the reason to hydrophilicity of such substrate. Therefore the highly increased surface area of the 5 s plasma treated silicon along with the large number of hydrophilic groups leads to the immediate change of surface to hydrophilic during contact angle measurement (Figure 1); in 90 s plasma treated sample, however, it takes longer for the surface to become hydrophilic due to lower concentration of OH^- groups and smaller surface area.

In conclusion, we found that hydrophilic chemical groups such as hydroxides were created on the silicon or silicon oxide surface through the controlled plasma treatment and fluidic SWNT dip-coating process. Also, nanoscale rough surface structures formed during the plasma treatment significantly increased the proximity of hydroxyl functional groups on the surface. These combined chemical and physical enhancements that attract the aqueous SWNT solution effectively enable us to build highly organized and very large scale SWNT network architectures in various dimensions and geometries. These results will enable us to fabricate very large scale and highly organized SWNT networks that can be used in various applications such as SWNT interconnects, transistors, sensors, and flexible electronics.

Acknowledgment. This work was supported by the National Science Foundation Nanoscale Science and Engineering Center (NSEC) for High-Rate Nanomanufacturing. The authors also would like to thank Dr. Xugang Xiong at Northeastern University and Dr. Eunah Lee at Horiba Jobin Yvon Co for technical advice on assembly of SWNTs and Raman spectroscopy. Y.J.J. acknowledges the support from Semiconductor Research Corporation (SRC-CSR) and National Science Foundation (CMMI-0825864).

Supporting Information Available: Electrical characterization of the resulting SWNT structures along with narrow scan XPS spectra for Si 2p and O 1s and detailed explanation. This material is available free of charge via the Internet at http://pubs.acs.org.

JA8076523